Performance Comparison of Gain-Coupled and Index-Coupled DFB Semiconductor Lasers

Arthur J. Lowery, *Member, IEEE*, and Dalma Novak, *Member, IEEE*

Abstract—**Comprehensive numerical simulations with the transmission-line laser model (TLLM) are used to compare the behavior of gain-coupled DFB lasers with index-coupled DFB lasers fabricated from identical materials. These simulations compare slope efficiency, threshold current, spectra, small-signal modulation bandwidth, maximum-intrinsic modulation bandwidth, large-signal transient response and chirp, relative-intensity-noise (RIN) spectra, and feedback sensitivity for coherence collapse. In most cases gain-coupled lasers with additional index coupling have better performance than index-coupled lasers for a given material. However, high-coupling factor index-coupled lasers do have lower threshold currents, lower RIN levels, and lower sensitivity to external feedback than gain-coupled lasers, although spatial hole burning in these devices can be disadvantageous.**

I. Introduction

GAIN-COUPLED distributed-feedback (DFB) semiconductor lasers have a built-in periodic longitudinal modulation of their net optical gain [1]. This modulation produces a coupling between the forward- and backward-traveling optical waves, providing the feedback mechanism for lasing with a wavelength set by the period of the modulation. As was shown by Kogelnik and Shank [2], this feedback prefers a single mode of oscillation. This preference for a single mode is in contrast to index-coupled DFB lasers, which have two degenerate modes of oscillation unless the waveguide has a perturbation in it such as a quarter-wave shift or a taper [3]. For this reason, there is currently much interest in gain-coupled DFB lasers.

Recent advances in fabrication technology have produced pure-gain-coupled lasers [Fig. 1(a)], [4]–[6], mixed-coupled lasers [Fig. 1(b)] [14], [5], [7], and loss-coupled structures with saturable loss [Fig. 1(c)] [8]–[11], or unsaturable loss [12], [13]. The devices have been fabricated from GaAlAs [4], [5], [13], MQW-GaAlAs [12], InGaAsP/InP [6], MQW-InGaAsP/InGaAs/InP [7]–[9], strained-layer MQW-GaInAlAs [10, 11] and strained-layer MQW-GaInAsP [14]. All these devices have some built-in longitudinal modulation of their net optical gain, and will be henceforth referred to as "gain-coupled" lasers. In contrast, "index-coupled," DFB lasers [Fig. 1(d)] have no built-in longitudinal modulation of optical gain. Gain-coupled lasers have been shown to have high single-mode yields [10]–[12], good side-mode suppression [7]–[12], – 3 dB modulation bandwidths better than 11 GHz at 10 mW [10], [11] and 12.8 GHz at 3 mW [14], low dynamic chirp [6], [13], [14], resistance to external feedback [15], and low mode-partition probability [9]. Also, Kudo *et al.* [16] have shown analytically that gain-coupled lasers with additional index coupling can have a reduced small-signal effective linewidth-enhancement factor (α-factor). Numerical simulations have shown that the large-signal effective α-factor can also be reduced [17], [18], and that the maximum intrinsic modulation bandwidth can be almost tripled in the same manner [19], [20].

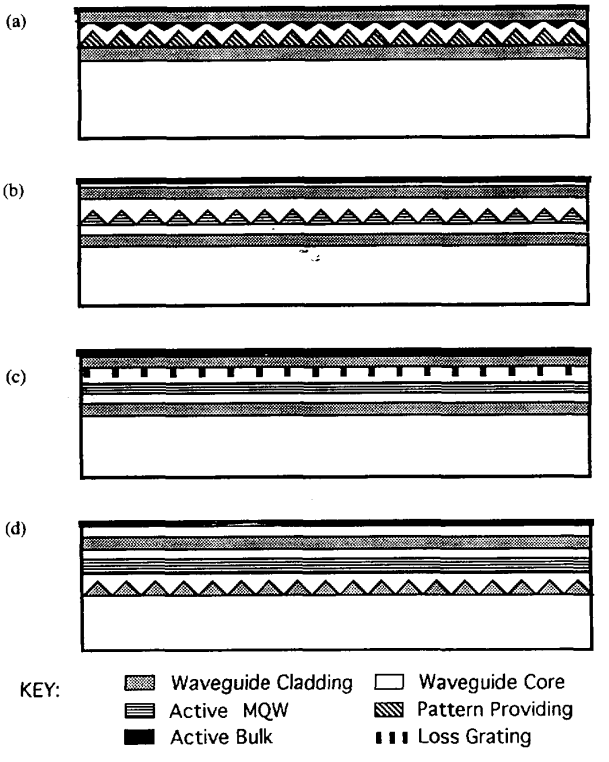

Fig. 1. Typical designs for DFB lasers: (a) pure gain coupled, (b) gain coupled with built-in index coupling, (c) gain coupled using a loss grating, (d) index coupled.

Manuscript received May 18, 1993; revised February 3, 1994. This work was supported by the Australian Photonics Cooperative Research Centre.

The authors are with the Photonics Research Laboratory, Department of Electrical Engineering, University of Melbourne, Vict. 3052, Australia.

IEEE Log Number 9402516

Although the above results indicate that gain coupling is a promising technology for laser fabrication, particularly since large as-cleaved single-mode yields are attainable [3], [12], a detailed performance comparison between gain-coupled lasers and index-coupled lasers manufactured from identical materials has yet to be made. Thus, it is uncertain whether gain-coupled lasers made using similar material technology to index-coupled lasers would out-perform the index-coupled lasers.

In this paper we present extensive numerical comparisons between index-coupled [as shown in Fig. 1(d)] and gain-coupled structures [as shown in Fig. 1(a) and (b)] fabricated from the identical materials. In our simulations the magnitude of the gain modulation is assumed to be dependent on carrier density, and therefore our results do not apply to loss-coupled devices [Fig 1(c)]. Our results are as follows.

- Index-coupled lasers offer lower threshold currents for high coupling ratios, noting that these devices can suffer from spatial hole burning causing nonlinearity in the light–current (L–I) characteristic.
- Gain-coupled lasers have single-mode optical spectra with high side-mode suppression ratios even when index coupling is introduced into the structure.
- The small-signal modulation response of gain-coupled lasers can be improved significantly with the addition of index coupling into the device. When the ratio of index to gain coupling is optimized, the -3 dB modulation bandwidth is over 11 GHz, compared with 7 GHz for an index-coupled laser with a high coupling factor at the same output power, and 6.5 GHz for gain-coupled lasers with no index coupling. The maximum intrinsic modulation bandwidth can be similarly improved.
- The large-signal response to digital modulation is significantly affected by the ratio of gain coupling to index coupling in gain-coupled lasers. The damping of the transient and the pulse width can be reduced using antiphase coupling, and increased using in-phase coupling.
- Gain-coupled lasers with additional index coupling have a slowly varying frequency shift (chirp) that occurs during large-signal transients. We demonstrate that this chirp is a result of longitudinal spatial hole burning (SHB) and that the sense of this chirp component is dependent on the relative phase of the index and gain gratings. In some cases the new chirp component can cancel the dynamic chirp.
- Because the K-factor [19] can be reduced using antiphase index coupling, antiphase coupling can reduce the low-frequency intensity noise (RIN) over that in pure-gain-coupled lasers. However, the RIN is no better than for index-coupled lasers with a high coupling coefficient.
- Gain-coupled lasers are more sensitive to external feedback than high-coupling index-coupled lasers, but less sensitive than low-coupling index-coupled lasers. Coherence collapse occurs at about -49 dB feedback for pure-gain-coupled lasers.

The paper is organized as follows. Section II discusses the numerical model. Section III includes a large number of comparisons between gain-coupled and index-coupled lasers, and Section IV concludes the paper.

II. Numerical Model

The transmission-line laser model (TLLM) [21] was chosen for these simulations because it can be used to simulate both gain-coupled [22] and index-coupled structures [23], [24] using the same object code, and is able to output a wide range of standard laser measurements including time-averaged optical spectra, small-signal frequency responses, large-signal transient responses, large-signal transient spectra, RIN spectra, and intensity fluctuations. The model can also be interfaced with models of delayed external reflections to assess feedback sensitivity.

The TLLM is a large-signal time-domain modeling technique [21]. The optical waveguide is modeled by a transmission-line divided into sections; each section represents a longitudinal slice of the laser, as shown in Fig. 2. Scattering matrices within each section model the optical properties of that section by modifying the optical traveling fields at each iteration, then passing the fields to the next section via lossless transmission lines that represent the optical propagation delays along the cavity. The transmission-line delays also allow the cavity field to be solved explicitly, i.e., each scattering operation can be solved independently and the result of the scattering passed to the adjacent matrices for the next iteration. Without the delays the field would need to be solved implicitly, as with transfer-matrix models [25].

A. Development of a Scattering Matrix Representing Gain Coupling

In gain-coupled DFB lasers the gain (or loss) is deeply modulated, as shown in Fig. 2(a). This modulation gives a large variation in the imaginary component of the wave impedance, causing significant coupling between the forward- and backward-traveling waves [2]. To enable this gain coupling to be modeled, new scattering matrices have to be developed for the TLLM.

For index-coupled DFB lasers, real-valued scattering matrices at the model-section boundaries represent the reflections caused by the real impedance (index) discontinuities [23]. For gain-coupled lasers, scattering matrices at the section boundaries would require imaginary elements to represent the reflections caused by the imaginary impedance (gain) discontinuities. Since TLLM's propagate only real samples of the optical field, such imaginary-valued matrices cannot be used. A solution is to represent the ac-component of the spatial-gain modulation by lumped conductances, $G(n)\,\Delta L$, at the center of each model section n, as shown in Fig. 2 (b). Positive conductances are used to represent mean section power gain coefficients $g(n)$ lower than the mean laser gain coeffi-

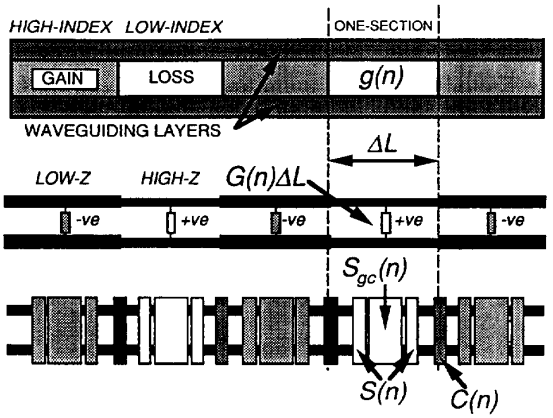

Fig. 2. Transmission-line laser model for gain-coupled lasers: (a) simplified structure to be modeled; (b) transmission-line equivalent including real-impedance modulation represented by the modulated characteristic impedance of the lines, and imaginary-impedance modulation represented by lumped conductances across the lines; (c) transmission-line equivalent using scattering matrices to represent the scattering at the impedance discontinuities.

cient over the entire laser length, g_{mean}. This method works because a positive conductance will absorb power. Conversely, negative conductances are used to represent mean section gains $g(n)$ higher than the mean laser gain. Each conductance causes reflections and thus coupling of the traveling waves. The coupling can be represented by *real-valued* scattering matrices, $S_{gc}(n)$ at the section centers. This real-valued scattering is equivalent to the desired imaginary-valued scattering at the boundaries, because the boundary–center–boundary phase-shift is 90° at the Bragg frequency, at which the model lases.

In TLLM's, the lasing frequency is down-converted in frequency to allow large iteration time steps to be used, to give realistic computing times [21]. Thus only a few scattering matrices are required to represent many periods of gain–loss in the laser, as in TLLM's of index-coupled lasers [23]. The Bragg frequency becomes $1/(4\,\Delta T)$, where ΔT is the iteration time step, and is equal to the propagation time of the optical waves across one section, length ΔL. Details regarding the effect of reducing the number of sections on the Bragg grating transmission spectrum are given in [23].

The amplification caused by the mean gain, g_{mean} can be represented by further scattering matrices, $S(n)$, placed just around $S_{gc}(n)$, shown in Fig. 2(c) [22]. However, for an efficient algorithm $S_{gc}(n)$ is normalized to be energy conserving, so that $g(n)$ is solely represented by $S(n)$. Index coupling can be also included in the model by further scattering, $C(n)$ at the section boundaries, as is detailed in [23].

The elements with the scattering matrices for gain can be derived in the following manner. The conductance of a model section, $G(n)\,\Delta L$ is found by equating the reflection coefficient at the conductance to the gain-coupling factor, $\kappa_g(n)\,\Delta L$ of each section. For a transmission line with impedance, Z_0 and $g(n)Z_0 \ll 1$, this gives

$$G(n)Z_0 = -2\kappa_g(n). \tag{1}$$

An energy-conserving scattering process for the gain coupling, $S_{gc}(n)$ can be derived for section n using Thévenin equivalents of the transmission lines and substituting (1):

$$\begin{bmatrix} A(n) \\ B(n) \end{bmatrix}_k^r = \frac{1}{\sqrt{1 + \left(\kappa_g(n)\,\Delta L\right)^2}} \cdot \begin{bmatrix} 1 & \kappa_g(n)\,\Delta L \\ \kappa_g(n)\,\Delta L & 1 \end{bmatrix} \times \begin{bmatrix} A(n) \\ B(n) \end{bmatrix}_k^i. \tag{2}$$

Here, A represents the forward-traveling wave and B represents the backward-traveling wave both normalized so that the optical intensity $= |A|^2$; i denotes waves incident upon the conductance node, r denotes reflected waves from the conductance nodes, and k is the iteration number [23].

The coupling within a model section can be related to the section gain by considering the sum of the in-phase reflections caused by the imaginary impedance discontinuities due to the *square-wave* modulation of the gain in the real device. The magnitude of the imaginary impedance discontinuities is easily related to the modulation depth of the gain by standard transmission-line formulas. For a square-wave modulation of gain and a first-order grating, transmission-line theory gives [26]

$$\kappa_g(n) = (g(n) - g_{\text{mean}})/\pi. \tag{3}$$

The gain, hence the scattering elements at each section, are recalculated from the local carrier density at each iteration. The use of a local carrier density means that longitudinal spatial hole burning (SHB) is included in the model. The iteration process simply comprises calculating the scattering at the section centers, passing the wave amplitudes to the section boundaries, calculating the connection at the boundaries, then passing the wave amplitudes back to the scattering matrices at the centers of the sections for the next iteration.

At each iteration and within each section, the carrier density is recalculated accounting for stimulated and spontaneous recombination, and current injection. In the gain-coupled model, the stimulated recombination within a section is calculated from the integral of the power density along the section, where the power density is calculated from the optical standing wave. In the index-coupled laser model, the standing wave is not used in the stimulated-recombination calculation, as it is assumed that the microscopic variations in carrier density would be washed-out by carrier diffusion. Such diffusion is blocked by the passive regions in the gain-coupled device.

Unlike our previous work [17], [19], [22], we have considered the optical standing wave when calculating the effect of the nonlinearity of the optical gain, represented by the gain-compression factor (ϵ). Because the maximum gain compression occurs at the peaks of the standing wave, where the maximum stimulated emission also oc-

curs, the effect of the gain nonlinearity is enhanced [27]. The inclusion of this effect allows for a fair comparison of the index- and gain-coupled lasers, because the gain-compression factor now has a consistent definition, i.e., ϵ is defined as that measured in a traveling-wave situation, such as in a laser amplifier.

B. Calculation of the Index- and Gain-Coupling Coefficients

The model is self-consistent; that is, the model iterates towards a solution of the carrier density in the active region that gives consistent values of threshold gain, gain coupling, and index coupling for a given refractive index in the passive region. In contrast, Zhang *et al.* choose an initial ratio of gain to index coupling [18]. Self-consistent values for the gain coupling, $\kappa_g L$ and the index coupling, $\kappa_i L$ were found by implementing the model with the parameters given in Table I, and are plotted against the passive region index step in Fig. 3. Also plotted is the coupling ratio, r of the index coupling to the gain coupling, where $r = \kappa_i/\kappa_g$. The passive region index step is defined as the passive region index minus the passive region index for pure gain coupling. The amount of index coupling is extremely sensitive to the passive region index, showing that purely gain-coupled lasers are difficult to fabricate in practice. A greater passive region index step is required to give a desired increase in $|\kappa_i|$ for antiphase coupling than for in-phase coupling. This is because for antiphase coupling, increasing $|\kappa_i|$ will lower the threshold-carrier density, increasing the index in the active region, thus decreasing the index difference between the active and passive regions, hence partially compensating the desired increase in $|\kappa_i|$.

III. Comparisons Between Gain-Coupled and Index-Coupled Lasers

The following results compare the performance of gain-coupled and index-coupled lasers with parameters as in Table I. Gain-coupled lasers with varying ratios of gain to index coupling were simulated in each comparison. All gain-coupled lasers were assumed to have a square-wave modulation of their longitudinal index and gain, although the results can be applied to other modulation forms by modification of (3). The index-coupled lasers were also assumed to have square-wave modulation of their index, and had quarter-wave shifts centrally placed in their gratings. Two coupling values (κL) were chosen for the index-coupled lasers: 1.25 and 3.0. A coupling of 1.25 gives minimum spatial hole buring [25].

A. Threshold Current and Slope Efficiency

The light–current (L–I) characteristics for gain-coupled and index-coupled DFB lasers were compared by letting simulations with a constant bias current run until the output power reached a steady state. In the case of the gain-coupled lasers, the current was assumed to be perfectly confined to the active material, with zero leakage through the passive regions. Fig. 4 shows the threshold current and slope efficiency for a gain-coupled laser

TABLE I
Laser Parameters

Symbol	Parameter Name	Value	Unit
λ	Grating Wavelength	1.55	μm
L	Laser Chip Length	300.0	μm
w	Active Region Width	3.5	μm
d	Active Region Depth	0.06	μm
N_0	Transparency Carrier Density	1.5×10^{18}	cm^{-3}
a	Gain Cross-Section	7.0×10^{-16}	cm^2
Γ	Confinement Factor	0.07	
ϵ	Gain compression factor	3.0×10^{-17}	cm^3
α	Linewidth Enhancement Factor	4.0	
$\bar{n}_e$	Group Index of Waveguide	3.75	
α_{sc}	Waveguide Attenuation Factor	20.0	cm^{-1}
R	Facet Reflectivities	0.0	%
B	Bimolecular Recomb. Coef.	1.0×10^{-10}	$cm^3.s^{-1}$
C	Auger Recomb. Coef.	3.0×10^{-29}	$cm^6.s^{-1}$
n_{sp}	Population inversion parameter	2.0	

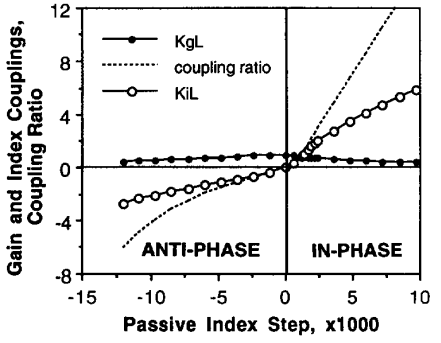

Fig. 3. Self-consistent gain κ_g and index κ_i coupling values and coupling ratio r versus passive index step for a gain-coupled laser.

against coupling ratio, calculated from L–I characteristics. Also shown are the threshold current and the slope efficiency of the two index-coupled lasers.

The results show that the threshold current for the gain-coupled lasers is lowest for large coupling ratios. This is because the total coupling (the geometric mean of the index and gain couplings) is increased with the addition of index coupling. The slope efficiency of the gain-coupled lasers decreases away from the $r = 0$ coupling ratio, but increases again at a coupling ratio of around -1.5. Although the $\kappa L = 3.0$ index-coupled laser has a low threshold current, this laser has the worst slope efficiency

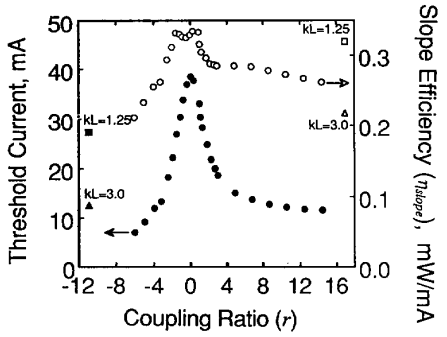

Fig. 4. Threshold current and slope efficiency for gain-coupled lasers with various coupling ratios.

and also suffers from nonlinearity caused by SHB [24], [25]. A better comparison is between the $\kappa L = 1.25$ laser and the $r = -1.53$ gain-coupled laser, which both have low SHB. These have similar efficiencies, thus, in terms of L–I characteristics gain-coupled lasers have no advantages over index-coupled lasers.

B. CW Spectral Characteristics

Although quarter-wave-shifted index-coupled lasers and gain-coupled lasers both have a dominant mode that guarantees single-mode operation, a conventional quarter-wave shifted DFB laser can suffer from SHB, which perturbs the grating and can lead to the appearance of a side mode [24], [25]. Because pure-gain-coupled lasers ($r = 0$) have a near-flat optical-field distribution, SHB is minimal in these lasers and so they should remain single mode even at high output powers. However, the spectral behavior of gain-coupled lasers when index-coupling is also present ($r \neq 0$) has not been theoretically studied and a detailed comparison of the spectral characteristics of mixed-coupled, gain-coupled, and conventional DFB lasers has yet to be presented.

To simulate the optical spectra for these lasers we iterated the model until CW conditions were obtained and then took a 16 384 point Fourier transform of the output optical field using a Blackman–Harris window function. The spectra were then convolved with a 0.1 nm FWHM Gaussian bell to obtain a spectrum similar to that which would be obtained experimentally with a grating–monochromator spectrum analyzer.

Fig. 5 shows the spectra of several gain- and index-coupled lasers. Pure gain coupling [Fig. 5(a)] gave a single dominant mode centrally placed within the stopband, as predicted analytically by Kogelnik and Shank [2]. The addition of index coupling did not degrade the side-mode suppression ratio [Fig. 5(b) and (c)], however the dominant mode shifted with respect to the stopband, as was observed by Luo *et al.* [5]. For antiphase coupling, the mode was at the blue end of the stopband: for inphase coupling the mode is at the red end of the stopband. Li *et al.* [7] have observed a similar spectrum to Fig. 5(c) for their mixed-coupled laser, indicating that their laser had a large amount of in-phase index coupling. Below threshold simulations [28] also show this behavior.

The index-coupled lasers with a quarter-wave shift also showed a single dominant mode centrally placed within the stopband [Fig. 5(d) and (e)]. In the case of the high-coupling-factor laser, spatial hole burning caused the appearance of a lower frequency side mode, marked "a" in Fig. 5(e). However, the side-mode suppression ratio is still over 40 dB, though the probability of mode hopping has been increased, giving the possibility of a noise floor in the bit-error rate characteristics of a fiber-transmission system [29]. This problem is reduced somewhat with MQW lasers because of the lower linewidth-enhancement factor [30].

C. Small-Signal Modulation Response

To date no comparisons have been made between the modulation responses of index- and gain-coupled lasers made from identical materials. However, numerical simulations of gain-coupled lasers have revealed that the maximum intrinsic modulation bandwidth, f_{max} calculated from the K-factor [31] as $f_{max} = 2\sqrt{2}\,\pi/K$, can be almost tripled by adjusting the ratio of index to gain coupling in a gain-guided laser [19]. Enhancement of the modulation bandwidth in an antiphase coupled laser was also predicted in [20]. Also, experimental measurements on gain-coupled lasers have shown -3 dB bandwidths of up to 12 GHz [14]. In comparison however, conventional structures with bandwidths of more than 17 GHz have also been reported [32].

Fig. 6 shows the simulated frequency responses of several gain- and index-coupled lasers at an optical output power of 5 mW. The highest resonant frequency of 7.3 GHz was obtained with an antiphase gain-coupled laser ($r = -1.53$), the lowest of 2.1 GHz with an in-phase gain-coupled laser ($r = 1.73$). The pure-gain-coupled laser ($r = 0$) had a resonant frequency of 5.6 GHz. The resonant frequencies of the index-coupled lasers were below those of the antiphase gain-coupled laser and the pure-gain-coupled laser, being 3.9 GHz for the $\kappa L = 1.25$ laser and 4.7 GHz for the $\kappa L = 3.0$ laser. This shows that gain-coupled lasers can give the highest resonant frequencies for a given material.

The standard expression for the small-signal resonant frequency, f_r of a semiconductor laser is [33]

$$f_r = \frac{1}{2\pi}\left(\frac{c\Gamma a_{eff}}{\bar{n}_e q w d L\, \eta_{slope}} P\right)^{1/2} \tag{4}$$

where P is the output power, η_{slope} is the slope efficiency (milliwatts/milliamp), A_{eff} is an effective gain cross-section, and the other parameters are as in Table I. For the index-coupled laser and assuming that the effective gain cross-section (a_{eff}) is almost equal to the material gain cross-section (a), this expression gives resonant frequencies of 4 GHz ($\kappa L = 1.25$) and 5 GHz ($\kappa L = 3.0$), in good agreement with the numerical simulations shown in Fig. 6. Equation 4 can also be used to calculate the effective gain

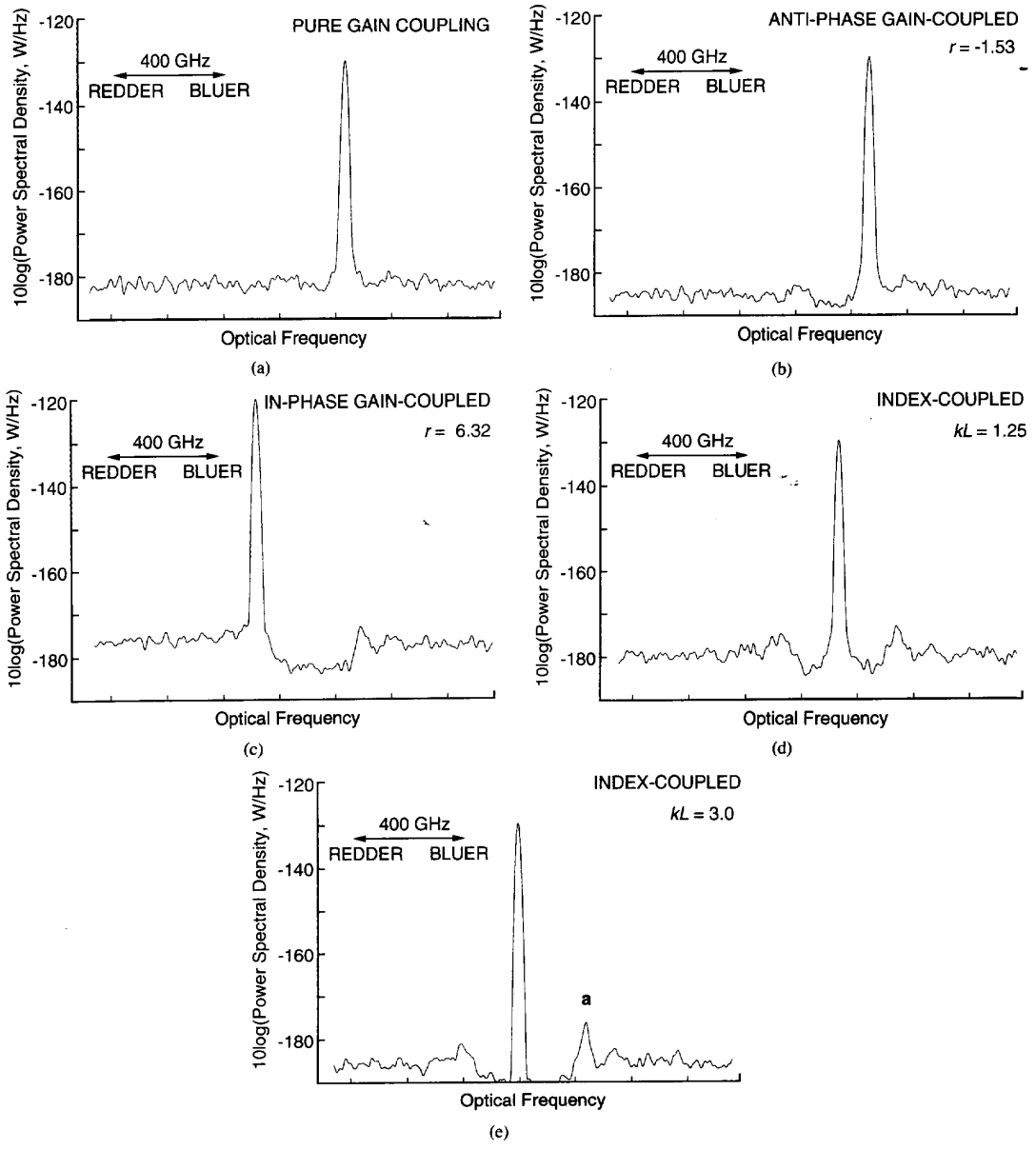

Fig. 5. Spectra of gain and index-coupled lasers. (a) Pure-gain-coupling; (b) gain coupling, coupling ratio = -1.53 anti-phase; (c) gain coupling, coupling ratio = 6.32 in-phase; (d) index coupling $\kappa L = 1.25$; (e) index coupling $\kappa L = 3.0$.

cross-section of gain-coupled lasers from the small-signal numerical simulations: the effective gain is $1.9a$ for pure gain coupling, $3.3a$ for $r = -1.53$, and $0.2a$ for $r = 1.73$. The increase in effective gain cross-section with antiphase couplings occurs because the Bragg reflection, due to the index coupling, increases when the carrier density in the gain regions of the laser is increased [16]. Hence, the optical gain change per carrier, including the mirror losses, is increased. Such a reduction is not seen in index-coupled DFB lasers because they are pumped homogeneously, or in loss-coupled devices where the loss is carrier independent.

We also investigated the variation of the -3 dB bandwidth of the gain-coupled lasers at 5 mW output power with coupling ratio, r (see Fig. 7). It is evident that the bandwidth can be increased to a maximum of 11.6 GHz using an antiphase coupling ratio close to -1.53 while the bandwidth of the pure-gain-coupled laser was 6.5 GHz. In contrast, in-phase couplings produce a marked decrease in modulation bandwidth, the minimum being 3.0 GHz at a coupling ratio of $r = 1.73$. The -3 dB bandwidths for the index-coupled lasers are also plotted in Fig. 7. These values are approximately equal to the modulation bandwidths for pure-gain-coupled structures, but are around

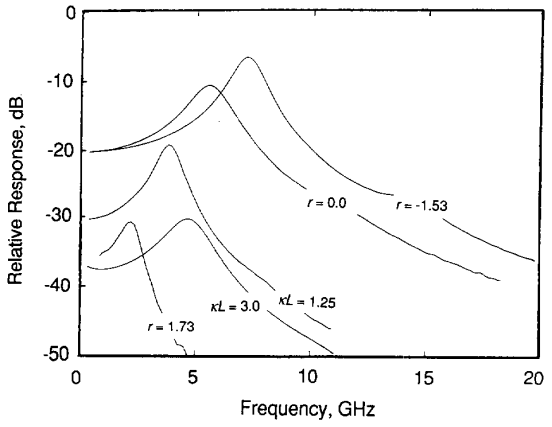

Fig. 6. Small-signal frequency responses of gain-coupled and index coupled lasers.

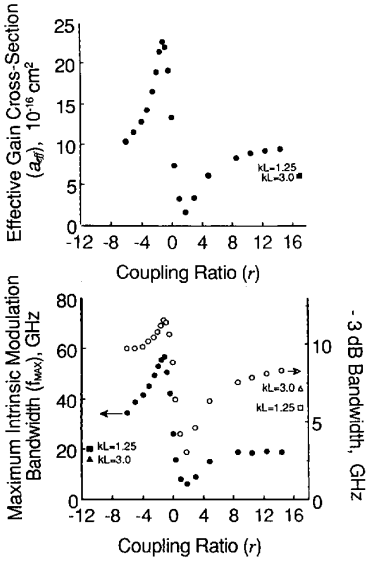

Fig. 7. Small-signal −3 dB bandwidth and maximum intrinsic modulation bandwidth and effective gain cross-section of gain-coupled and index-coupled lasers.

half the bandwidth of the optimum antiphase gain-coupled laser. The −3 dB modulation bandwidth of the gain-coupled laser displays a near-asymptotic behavior at large negative-coupling ratios, which is due to the combined effect of the slope efficiency (see Fig. 4) and the effective gain cross-section (also plotted in Fig. 7).

The maximum intrinsic modulation bandwidth, f_{max} of the lasers (obtained from the frequency response curves [31]) is also shown in Fig. 7. The optimum antiphase coupled laser has a maximum intrinsic modulation bandwidth of 57 GHz, over twice the value for the pure-gain-coupled laser and over triple the value for the $\kappa L = 3.0$ index-coupled laser. The maximum intrinsic modulation bandwidth falls to a very low value of 5.8 GHz for an in-phase coupling ratio of $r = 1.73$, which is a result of the very small effective gain cross-section. Comparison of the effective gain cross-section and the maximum intrinsic modulation bandwidth shows that they have similar trends, as expected for lasers with a near-constant photon lifetime [31].

D. Large-Signal Transient Response and Time-Resolved Chirp

To assess the performance of the lasers in digital systems, we simulated the dynamic response of the lasers in the previous section and then compared their time-resolved frequency waveforms. The lasers were driven with a pulsed waveform to produce a large-signal transient from a bias ("0"-symbol) power of 500 μW to a "1" symbol power of 5 mW. The symbol sequence was "001011" and the symbol period was 1 ns.

Fig. 8(a) shows the response of a laser with pure gain coupling. There is a transient during the first two 0's, due to the bias level being above threshold and the initial carrier density being below threshold. The 0 to 1 transition produces a large transient with a resonant frequency of $\approx$ 6 GHz. The second 0 to 1 transient is almost identical to the first, indicating that the carrier density and output-power conditions just before the two 0 to 1 transitions were similar. The upper trace in Fig. 8(a) is the time-resolved frequency of the pulses. This was obtained by taking a fast Fourier transform (FFT) of the optical output field over a 6 ps window, plotting the peak frequency of the transform, then advancing the transform window by 0.18 ps to find the next peak frequency. There was a strong blue–red chirp during all of the transient optical pulses, which is the usual dynamic chirp. There is also a small offset between the mean frequency during the 0 symbols and the 1 symbols. This is the adiabatic chirp due to the change in threshold carrier density (hence refractive index) with output power because of nonlinear gain [34].

Fig. 8(b) shows the response of an in-phase coupled laser with $r = 1.73$. The transients during the 1 symbols are heavily damped and the relaxation frequency is $\approx$ 2.5 GHz. The time-resolved frequency shows that the adiabatic chirp is large as expected from the very small effective gain cross-section, a_{eff}. However, there is also a new component to the chirp which, when added to the adiabatic chirp, causes a *slow* drift in mean frequency between 1 and 0 symbols, as though the adiabatic chirp has been low-pass filtered. This slow drift cancels the blue–red dynamic chirp of the first transient pulse of the 1 symbols. The new chirp component in also apparent during the 1–0 frequency transient, and from this has a time constant of between 200 and 400 ps.

Fig. 8(c) shows the output-power waveform for a laser with an antiphase coupling of $r = -1.53$. The transient pulses have large amplitudes, and the resonance frequency during 1 symbols is $\approx$ 8 GHz, as expected from the small-signal simulations. The time-resolved frequency has the usual dynamic chirp, but the long-term frequency shift between the 1 and 0 symbols exhibits the opposite

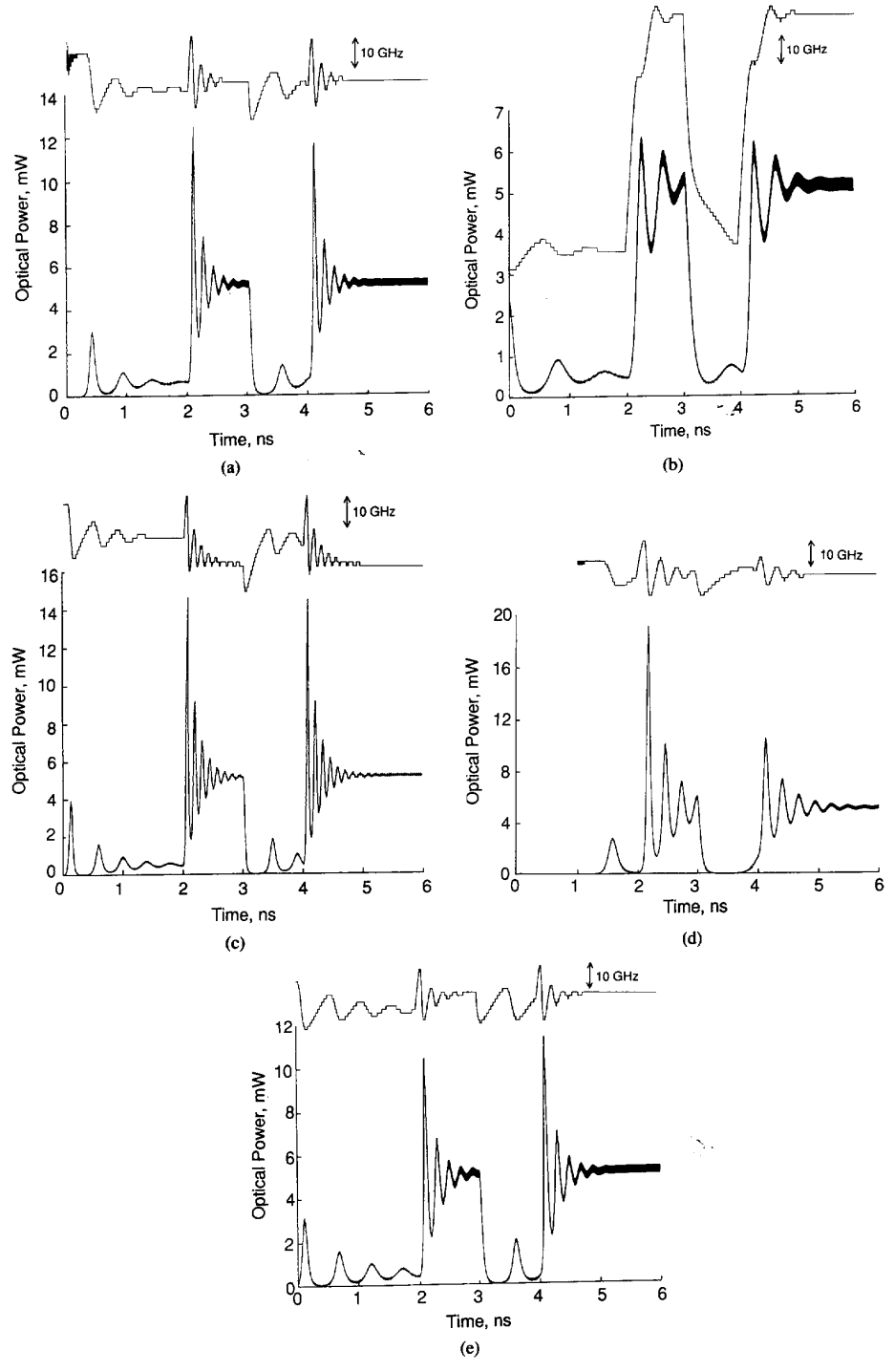

Fig. 8. Large-signal transient responses and time-resolved spectra for a 001011 modulation symbol sequence. (a) Pure gain coupling; (b) gain-coupling, coupling ratio = 1.73 in-phase; (c) gain coupling, coupling ratio = −1.53 anti-phase; (d) index-coupling $\kappa L = 1.25$; (e) index-coupling $\kappa L = 3.0$.

sign to that expected for adiabatic chirp resulting from nonlinear gain. This again suggests a new chirp component, which is dominant over the usual adiabatic chirp and has the opposite sign to that in the in-phase-coupling laser. Usually, the dynamic chirp oscillates about a mean frequency set by the adiabatic chirp for that power level as in Fig. 8(a). However the slow increase of the new chirp component causes the mean optical frequency to drift to the red during the 0–1 transient ringing. Fig. 8(d) and (e) are the transient responses and time-resolved spectra for index-coupled lasers with $\kappa L = 1.25$ and $\kappa L = 3.0$, respectively. These have similar features to those of the gain-coupled lasers, including transient pulses during the 0 symbols in the $\kappa L = 3.0$ laser, which are caused by a recovery of the spatial hole burning lowering the lasing threshold during the 0 symbols.

Fig. 9 summarizes the magnitude of the new chirp for gain-coupled lasers with a wide range of coupling ratios r. The new chirp magnitude was measured from the mean point of the blue–red shift during the first relaxation pulse of a 1 symbol, to the steady-state frequency during a 1 symbol. The trace shows that for all antiphase couplings the new chirp component has a negative magnitude. The drift is positive for most in-phase couplings, and maximum for a coupling ratio close to 2.6, where the effective gain cross-section is a minimum. Fortunately, the new chirp component is less than 10 GHz at $r = -1.53$, the ratio giving the highest resonant frequency.

The time constant of the new chirp component is in the order of the differential carrier lifetime (350 ps), suggesting that the dynamics of longitudinal SHB could be the origin of the new chirp in the gain-coupled lasers [35]. To test whether SHB was present we plotted in Fig. 10 the carrier density during the simulations of Fig. 8 with bars to indicate the difference between the maximum and minimum carrier densities along the laser cavity at a given time. The pure-gain-coupled laser shows very little spatial hole burning of the carrier density [Fig. 10(a)]. In contrast, the in-phase coupling laser [Fig. 10(b)] had SHB during 1 symbols, and approximately half the amount of SHB during 0 symbols. There is a large difference in threshold carrier density between the 0 and 1 symbols, which can be partially attributed to SHB at the center of the laser increasing the index coupling at the center of the laser, which increases the threshold carrier density, and partially attributed to nonlinear gain. Because the SHB takes time to "burn-in" during the 0–1 transients and to "recover" after the 1–0 transients, as can be seen in Fig. 10(b), the SHB-induced component of the threshold-carrier density change is not instantaneous. Furthermore, comparison of Figs. 8 and 10 shows that the time-resolved frequency is approximately proportional to the instantaneous mean carrier density. Therefore, because the dynamics of the new chirp component are similar to the dynamics of the SHB-induced change in mean carrier density, the new chirp component is likely to be caused by the SHB. A similar SHB-induced chirp caused by a long-term variation in threshold carrier density due to spatial hole burning occurs in the high-coupling index-coupled DFB laser [Fig. 10(e)], as has been investigated previously by Kinoshita and Matsumoto [35].

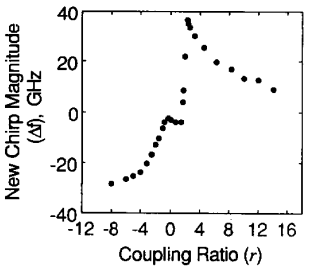

Fig. 9. Frequency shift during 0–1 transient caused by SHB-component of chirp versus coupling ratio.

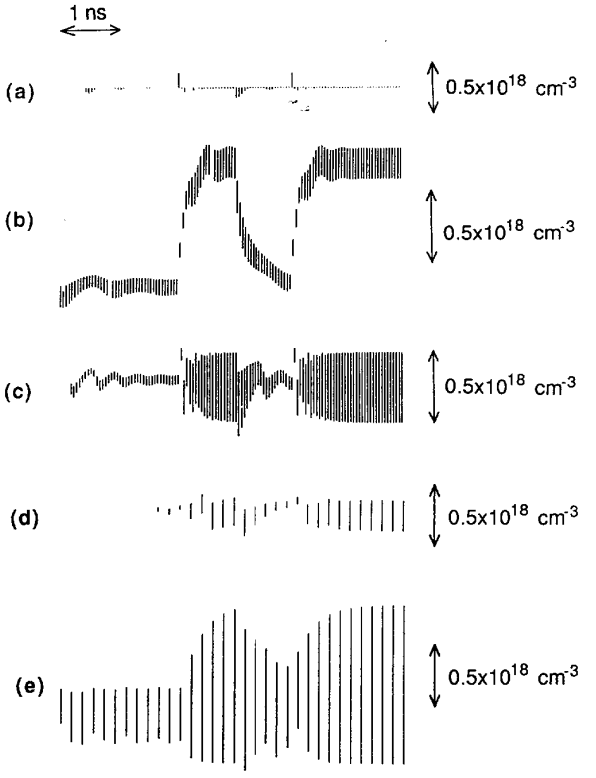

Fig. 10. Carrier-density evolution during modulation sequences shown in Fig. 8.

Fig. 10(c) shows the SHB in a laser with antiphase coupling. Fig. 8(c) showed that the frequency of 1 symbols is lower than for 0 symbols for this laser, which is commensurate with the lower mean carrier density during 1 symbols seen in Fig. 10(c). One reason why the carrier density drifts to lower levels during 1 symbols could be SHB at the center of the laser. Because of the phase of the index grating, the index coupling at the center of the laser is decreased by the SHB of the carrier density, allowing more light to couple to the ends of the laser

cavity. Thus, the light sees the higher (undepleted) gain near the ends of the laser. The result is a reduction in the threshold gain, and the threshold carrier density is reduced accordingly, leading to the negative frequency shift. The time constant of the SHB is similar to the time constant of the frequency drift, confirming SHB to be a likely cause of the new chirp component in gain-coupled lasers.

E. Relative Intensity Noise

The relative intensity noise (RIN) is particularly important in analog television transmission systems where a high detected signal-to-noise ratio is required. For a system with a low fiber loss, the RIN is the ultimate limit to the detected signal-to-noise ratio. Fukushima *et al.* [36] showed theoretically that the RIN at low frequencies is proportional to the square of the K-factor at powers of a few milliwatts, assuming a constant laser linewidth, and demonstrated a reduction in RIN in lasers with low K-factors. Thus, gain-coupled lasers with some index coupling should have a lower RIN than conventional lasers because of their high intrinsic modulation bandwidths, and hence, low K-factors.

To test the above hypothesis, the RIN was simulated for a number of laser types for an output power of 5 mW. The RIN was obtained by modeling the lasers with a constant bias current for the equivalent of 7 ns and then Fourier transforming the detected photocurrent to obtain the intensity-noise spectrum. The relative intensity noise was then obtained by dividing the intensity noise spectrum by the square of the mean photocurrent. Because the TLLM is noise driven, the intensity-noise spectrum is noisy, and so was smoothed by convolution with a 500 MHz FWHM Gaussian function. This smoothing is similar to reducing the video bandwidth on an RF spectrum analyzer.

Fig. 11 shows the RIN spectra for the gain-coupled and index-coupled lasers. As expected, the peak RIN occurs at the small-signal resonant peak for each device [36]. The $r = 0$ and the $r = 1.73$ gain-coupled lasers, and the $\kappa L = 1.25$ index-coupled laser have peak RIN levels close to -103 dB/Hz. However, because of the higher resonant frequency of the pure-gain-coupled laser, the RIN close to dc is reduced by about 5 dB compared with the in-phase-coupling device. The addition of antiphase index coupling further reduces the RIN by another 6 dB. Thus, the low K-factors of the antiphase gain-coupled laser do reduce the RIN levels close to dc. However the lowest RIN level is obtained with the $\kappa L = 3.0$ index-coupled laser, which is due to its low threshold gain, hence low spontaneous-emission rate.

F. Sensitivity to External Feedback

One widely reported effect of feedback from -50 to -10 dB is coherence collapse; "coherence collapse" refers to a large broadening of the laser's linewidth to tens of gigahertz [37]–[39]. Accompanying the massive broadening is an increase in intensity noise [40] and a chaotic

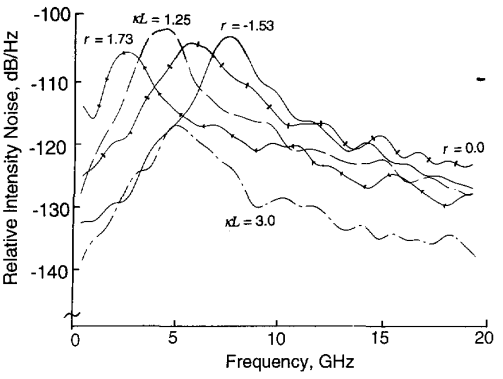

Fig. 11. Relative-intensity-noise (RIN) spectra for gain-coupled and index-coupled lasers.

intensity waveform [41]. Coherence collapse is detrimental to the operation of most optical communication systems. The TLLM has been shown to be accurate in the regimes of coherent feedback in Fabry–Perot lasers [42]. Here we compare the sensitivity of index-coupled lasers to coherence collapse with that of gain-coupled structures. We do this by measuring the intensity noise over a given bandwidth, then increasing the feedback level until there is a rapid increase in intensity noise. The intensity noise was estimated by taking the standard deviation of the output power after the output power was smoothed using a moving average of 100 iterations. This is equivalent to integrating the intensity noise spectrum over a bandwidth of approximately 33 GHz.

Fig. 12 shows the rms intensity noise versus feedback level for several gain- and index-coupled lasers. All of these curves show a clear transition to a chaotic regime at some threshold level of feedback, and a near-constant level of noise below this threshold. We define the threshold as the feedback level where the intensity noise is 1 mW rms. The $\kappa L = 1.25$ index-coupled laser has the lowest threshold level (-55 dB), followed by the pure-gain-coupled laser and the antiphase gain-coupled laser (both around -49 dB). The $\kappa L = 3.0$ index-coupled laser had the highest threshold (-27 dB). Favre [43] has used a feedback-sensitivity parameter, C to quantify the change in the complex propagation constant within the laser when there is external feedback. He has shown that the relative feedback sensitivity (dB) is approximately 28.5 $\log_{10}$ (ratio of coupling factors). Therefore the $\kappa L = 1.25$ laser should have a sensitivity to feedback 10.8 dB higher than that of the $\kappa L = 3.0$ laser. Our results give a difference between the coherence-collapse threshold of these devices as 27 dB. Therefore, the feedback-sensitivity parameter is not a good indication of coherence-collapse feedback threshold. However, Favre's conclusion that the feedback sensitivity of gain-coupled lasers is dependent on the total coupling, and is therefore comparable with index-coupled lasers, appears to be valid.

Fig. 13 shows the intensity waveforms, obtained by squaring the optical field and averaging over 100 itera-

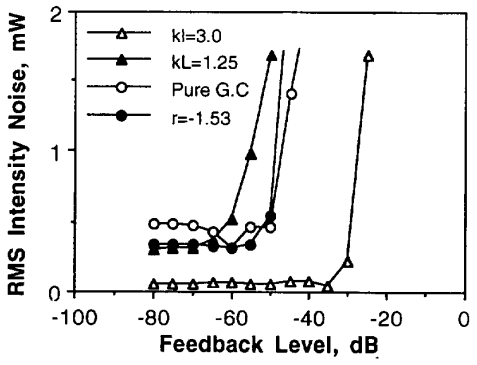

Fig. 12. Intensity noise versus external feedback level for four types of laser.

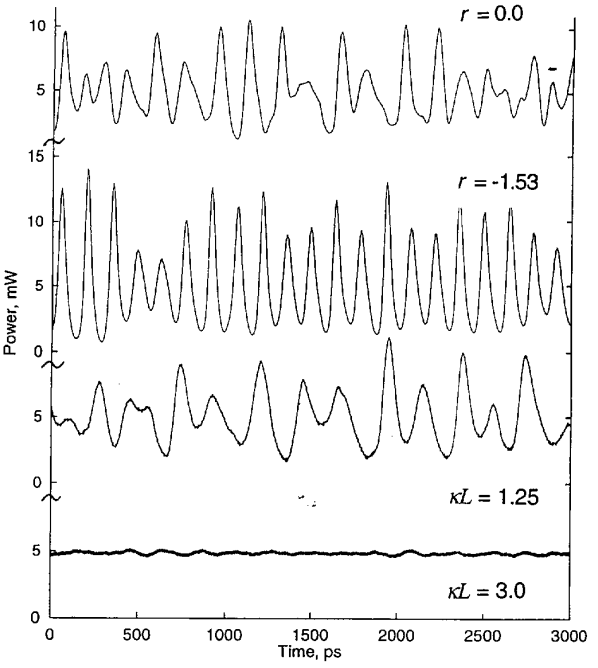

Fig. 13. Intensity waveforms at −40 dB feedback for the lasers in Fig. 12.

tions, for −40 dB feedback for the four lasers studied in Fig. 12. For the pure-gain-coupled laser [Fig. 13(a)] and the $\kappa L = 1.25$ index-coupled laser [Fig. 13(c)] the intensity behaved chaotically, with a modulation depth of almost 100 percent. In the case of the antiphase-coupled laser [Fig. 13(b)], the intensity showed a large amplitude resonance at 7 GHz, close to the resonant frequency of the laser, rather than the expected chaotic behavior. This resonance is probably large because of the low damping factor for this coupling ratio. In contrast, the $\kappa L = 3.0$ laser [Fig. 13(d)] shows only small intensity fluctuations at this feedback level.

IV. Discussions and Conclusions

In Section III we performed a detailed comparison between the performance of gain-coupled and index-coupled lasers and have shown the following.

- Pure-gain-coupled lasers have similar L–I characteristics to index-coupled structures with low coupling. High-coupling index-coupled structures have a lower threshold current than gain-coupled lasers, which have been optimized for large modulation bandwidth; however, they can exhibit a nonlinear characteristic caused by spatial hole burning, and the possibility of increased intersymbol interference in digital systems.
- Gain-coupled lasers offer a stable single-mode output, similar to that obtained with phase-shifted index-coupled structures. However, gained-coupled structures do not suffer from the severe SHB that occurs in high-coupling quarter-wave-shifted DFB lasers. This spatial hole burning can cause multimoded behavior at higher powers.
- Addition of antiphase index-coupling to gain-coupled lasers enhances the resonant frequency in gain-coupled lasers. Furthermore, the maximum intrinsic modulation bandwidth for gain-coupled lasers with index coupling is much greater than that obtained with index-coupled lasers fabricated from identical materials and operating at similar output powers. Thus, if parasitics are minimized, gain-coupled lasers offer improved modulation bandwidths in both analog and digital lightwave systems.
- Gain-coupled structures with optimized index coupling and index-coupled lasers offer similar performance in lightwave systems with regard to transient response and chirp. However, in-phase coupled lasers can suffer from a large SHB-induced chirp, and high-coupling index-coupled lasers can suffer from pulses during 0 symbols when the SHB recovers. The best lasers in terms of chirp and fast modulation response are the antiphase-coupled gain-coupled lasers with a coupling ratio of −1.53.
- The RIN in gain-coupled lasers can be reduced by the addition of antiphase index coupling. This is because the RIN is proportional to the K-factor squared, assuming a constant linewidth [36]. Greater than 6 dB improvement in RIN noise was obtained for an antiphase gain-coupled laser with $r = -1.53$, over the RIN of a pure-gain-coupled laser. However, the RIN of the pure-gain-coupled laser was found to be higher than in high-coupling index-coupled lasers due to its higher threshold gain.
- Gain-coupled lasers appear to be more sensitive to external feedback than high-coupling index-coupled lasers in terms of coherence collapse. However, an antiphase gain-coupled laser with $r = -1.53$ is more tolerant to feedback than an index-coupled laser designed for minimum spatial hole burning, but has a

strong resonant output in the coherence-collapsed state.

One important conclusion is that the effective gain can be maximized in gain-coupled lasers with the addition of antiphase index-coupling, and that this increase in gain can increase the maximum intrinsic modulation bandwidth, the resonance frequency, and the -3 dB bandwidth, and can decrease the dynamic chirping, the RIN noise, and the sensitivity to external feedback. Fortunately, the optimum mix of gain and index coupling is the same for each of these parameters ($r = -1.53$), because they are all dominated by the effective gain cross-section, a_{eff}. Thus the calculation of Kudo *et al.* of an increased effective gain cross-section for gain-coupled lasers with antiphase index coupling has far wider implications than just reducing the small-signal chirp factor of gain-coupled lasers.

The overall conclusion is that gain-coupled lasers perform better than index-coupled lasers in most situations. However, index-coupled lasers with high-coupling factors do have the lowest sensitivity to external feedback, although they also suffer from SHB, which can lead to nonlinear L–I characteristics, side modes and mode-partitioning, pulsing during zero symbols, and wavelength drift during 1 symbols. Although gain-coupled lasers with index coupling also suffer from spatial hole burning, the effect of SHB on their performance is small if the gain cross-section is optimum for a low chirp and a high resonant frequency.

References

[1] Y. Luo, Y. Nakano, K. Ikeda, K. Tada, T. Inoue, H. Hosomatsu, and I. Iwaoka, "Low threshold CW operation in a novel gain-coupled distributed feedback laser," *Tech. Dig. 12th IEEE Int. Semiconduct. Laser Conf.*, Davos, Switzerland, paper E-6, pp. 70–71, 1990.

[2] H. Kogelnik and C. V. Shank "Coupled-wave theory of distributed feedback lasers," *J. Appl. Phys.*, vol. 43, pp. 2327–2335, 1972.

[3] K. David, G. Morthier, P. Vankwikelberge, R. G. Baets, T. Wolf, and B. Borchert, "Gain-coupled DFB lasers versus index-coupled and phase-shifted DFB lasers: A comparison based on spatial hole-burning corrected yield," *IEEE J. Quantum Electron.*, vol. 27, pp. 1714–1723, 1991.

[4] Y. Luo, Y. Nakano, K. Tada, T. Inoue, H. Hosomatsu, and H. Iwaoka, "Purely gain-coupled distributed feedback semiconductor lasers," *Appl. Phys. Lett.*, vol. 56, pp. 1620–1622, 1990.

[5] ——, "Fabrication and characteristics of gain-coupled distributed feedback semiconductor lasers with a corrugated active layer," *IEEE J. Quantum Electron.*, vol. 27, pp. 1724–1731, 1991.

[6] S. Nakajima, T. Inoue, Y. Luo, T. Oki, Y. Nakano, K. Tada, R. Takahashi, and T. Kamiya, "Dynamic characteristics of 1.55 μm gain-coupled distributed feedback laser," *Conf. Dig. 13th IEEE Int. Semiconduct. Laser Conf.*, Takamatsu, Japan, paper B-4, pp. 18–19, Sept. 21–25, 1992.

[7] G. P. Li, T. Makino, R. Moore, and N. Puetz, "1.55 μm index/gain coupled DFB lasers with strained layer multiquantum-well active grating," *Electron. Lett.*, vol. 28, pp. 1726–11727, 1992.

[8] W. T. Tsang, F. S. Choa, M. C. Wu, Y. K. Chen, R. A. Logan, S. N. G. Chu, and A. M. Sergent, "Semiconductor distributed feedback lasers with quantum well or superlattice gratings for index or gain-coupled optical feedback," *Appl. Phys. Lett.*, vol. 60, pp. 2580–2582, 1992.

[9] W. T. Tsang, F. S. Choa, M. C. Wu, Y. K. Chen, R. A. Logan, T. Tanbun-Ek, S. N. G. Chu, A. M. Sergent, P. Magill, R. Reichmann, and C. A. Burrus, "Gain-coupled long wavelength InGaAsP/InP distributed feedback lasers with quantum-well gratings grown by chemical beam epitaxy," *Conf. Dig. 13th IEEE Int. Semiconduct. Laser Conf.*, Takamatsu, Japan, paper B-1, pp. 12–13, Sept. 21–25, 1992.

[10] B. Bourchert, B. Stegmüller, R. Gessner, and I. Kargner, "1.58 μm GaInAlAs SL-QW gain-coupled (GC) DFB lasers with high performance," *Conf. Dig. 13th IEEE Int. Semiconduct. Laser Conf. (postdeadline session)*, Takamatsu, Japan, paper PD-10, pp. 19–20, Sept. 21–25, 1992.

[11] B. Bourchert, B. Stegmüller, and R. Gessner, "Fabrication and characteristics of improved strained quantum-well GaInAlAs gain-coupled DFB lasers," *Electron. Lett.*, vol. 29, pp. 210–211, 1993.

[12] H-L. Cao, Y. Nakano, K. Tada, Y. Luo, M. Dobashi, and H. Hosomatsu, "Low threshold and high single-mode yield MQW gain-coupled DFB laser," *Tech. Dig. 4th Optoelectron. Conf. (OEC'92)*, Makuhari Messe, Japan, paper PD-3, pp. 6–7, July 1992.

[13] Y. Luo, H.-L. Cao, M. Dobashi, H. Hosomatsu, N. Nakano, and K. Tada, "Gain-coupled DFB laser diode using novel absorptive conduction-type-inverted grating," *Conf. Dig. 13th IEEE Int. Semiconduct. Laser Conf.*, Takamatsu, Japan, paper B-2, pp. 14–15, Sept. 21–25, 1992.

[14] C. E. Zah, P. J. Delfyett, R. Bhat, C. Caneau, F. Faivre, B. Pathak, P. S. D. Lin, A. S. Gozdz, N. C. Andreadakis, M. A. Koza, M. Z. Iqbal, H. Izapandra, and T. P. Lee, "High-speed performance of 1.5 μm compressive-strained multiple-quantum-well gain-coupled distributed-feedback lasers," *Tech. Dig. OFC/IOOC'93*, San Jose, CA, paper TuM4, pp. 61–62, 1993.

[15] Y. Nakano, Y. Deguchi, K. Ikeda, Y. Luo, and K. Tada, "Resistance to external optical feedback in a gain-coupled semiconductor DFB laser", *Tech. Dig. 12th IEEE Int. Semiconduct. Laser Conf.*, Davos, Switzerland, paper E7, pp. 72–73, 1990.

[16] K. Kudo, J. I. Shim, K. Komori, and S. Aria, "Reduction of effective linewidth enhancement factor, α_{eff}, of DFB lasers with complex coupling coefficient," *IEEE Photon. Technol. Lett.*, vol. 4, pp. 531–533, 1992.

[17] A. J. Lowery, "Large-signal effective α-factor of complex-coupled DFB semiconductor lasers," *Electron. Lett.*, vol. 28, pp. 2295–2296, 1992.

[18] L. M. Zhang, J. E. Carroll, and C. Tsang, "Dynamic response of the gain-coupled DFB laser," *IEEE J. Quantum Electron.*, vol. 29, pp. 1722–1727, June 1993.

[19] A. J. Lowery and D. Novak, "Enhanced maximum intrinsic modulation bandwidth of complex-coupled DFB lasers," *Electron. Lett.*, vol. 29, pp. 461–463, 1993.

[20] L. M. Zhang and J. E. Carroll, "Enhanced AM and FM modulation responses of complex coupled DFB lasers, " *IEEE Photon. Technol. Lett.*, vol. 5, pp. 506–508, May 1993.

[21] A. J. Lowery, "Transmission-line modeling of semiconductor lasers: The transmission-line laser model," *Int. J. Numer. Model*, vol. 2, pp. 249–265, 1990.

[22] A. J. Lowery and D. F. Hewitt, "Large-signal dynamic model for gain-coupled DFB lasers based on the transmission-line laser model," *Electron. Lett.*, vol. 28, pp. 1959–1960, 1992.

[23] A. J. Lowery "A new dynamic model for multimode-chirp in DFB semiconductor lasers," *IEE Proc. Pt., J.*, vol. 137, pp. 293–300, 1990.

[24] A. J. Lowery, C. N. Murtonen, and A. J. Keating, "Modeling the static and dynamic behavior of quarter-wave-shifted DFB lasers," *IEEE J. Quantum Electron*, vol. 28, pp. 1874–1883, 1992.

[25] J. E. Whiteaway, G. H. B. Thompson, A. J. Collar, and C. J. Armistead, "The design and assessment of $\lambda/4$ phase-shifted DFB structures," *IEEE J. Quantum Electron.*, vol. 25, pp. 1261–1279, 1989.

[26] K. David, J. Buus, and R. G. Baet, "Basic analysis of AR-coated, partly gain coupled DFB lasers: The standing-wave effect," *IEEE J. Quantum Electron.*, vol. 28, pp. 427–433, 1991.

[27] This theory has been presented by A. Sapia at the COST-240 Workshop on Model. Measurement Advanced Telecommun. Dev., Paris, France, Oct. 27, 1993.

[28] G. P. Li, T. Makino, R. Moore, N. Puetz, K.-W. Leong, and H. Lu,

"Partly gain-coupled 1.55 μm strained-layer multiquantum-well DFB lasers," *IEEE J. Quantum Electron.*, vol. 29, pp. 1736–1742, June 1993.

[29] N. Henmi, Y. Koizumi, M. Yamaguchi, M. Shikada, and I. Mito, "The influence of directly modulated DFB LD sub-mode oscillation on long-span transmission systems," *J. Lightwave Technol.*, vol. 6, pp. 636–642, 1988.

[30] K. Uomi, S. Sasaki, T. Tsuchiya, and M. Okai, "Spectral linewidth reduction by low spatial hole burning in 1.5 μm multi-quantum-well $\lambda/4$-shifted DFB lasers," *Electron. Lett.*, vol. 26, pp. 52–53, 1990.

[31] R. Olshansky, P. Hill, V. Lanzisera, and W. Powazinik, "Frequency response of 1.3 μm InGaAsP high speed semiconductor lasers," *IEEE J. Quantum Electron.*, vol. QE-23, pp. 1410–1418, 1987.

[32] K. Uomi, H. Nakano, and N. Chinone, "Ultrahigh-speed 1.55 μm $\lambda/4$-shifted DFB lasers with a bandwidth of 17 GHz," *Electron. Lett.*, vol. 25, pp. 668–669, 1989.

[33] K. Uomi, H. Nakano, and N. Chinone, "Intrinsic modulation bandwidth in ultra-high-speed 1.3 and 1.55 μm GaInAsP DFB lasers," *Electron. Lett.*, vol. 25, pp. 1689–1690, 1989.

[34] R. S. Tucker, "High-speed modulation of semiconductor lasers," *J. Lightwave Technol.*, vol. LT-3, pp. 1180–1192, 1985.

[35] J-I. Kinoshita and K. Matsumoto, "Transient chirping in distributed feedback lasers: Effect of spatial hole-burning along the laser axis," *IEEE J. Quantum Electron.*, vol. 24, pp. 2160–2169, 1988.

[36] T. Fukushima, R. Nagarajan, J. E. Bowers, R. A. Logan, and T. Tanbun-Ek, "Relative intensity noise reduction in InGaAs/InP multiple quantum well lasers with low non-linear damping," *IEEE Photon. Technol. Lett.*, vol. 3, pp. 691–693, 1991.

[37] D. Lenstra, B. H. Verbeek, and A. J. den Boef, "Coherence collapse in single-mode semiconductor lasers due to optical feedback", *IEEE J. Quantum Electron.*, vol. QE-21, pp. 674–679, 1985.

[38] R. W. Tkach, and A. R. Chraplyvy, "Regimes of feedback effects in 1.5 μm distributed feedback lasers," *J. Lightwave Technol.*, vol. LT-4, pp. 1655–1661, 1986.

[39] L. Goldberg, H. F. Taylor, A. Dandridge, J. F. Weller, and R. O. Miles, "Spectral characteristics of semiconductor lasers with optical feedback," *IEEE J. Quantum Electron.*, vol. QE-18, pp. 555–563, 1982.

[40] S. L. Woodward, T. L. Koch, and U. Koren, "The onset of coherence collapse in DBR lasers," *IEEE Photon. Technol. Lett.*, vol. 2, pp. 391–394, 1990.

[41] N. Schunk, and K. Petermann, "Numerical analysis of the feedback regimes for a single-mode semiconductor laser with external feedback," *IEEE J. Quantum Electron.*, vol. 24, pp. 1242–1247, 1998.

[42] A. J. Lowery, "A two-port bilateral model for semiconductor lasers," *IEEE J. Quantum Electron.*, vol. 28, pp. 82–92, 1992.

[43] F. Favre, "Sensitivity to external optical feedback for gain-coupled DFB semiconductor lasers," *Electron. Lett.*, vol. 27, pp. 433–435, 1991.

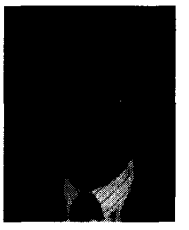

Arthur James Lowery (M'92) was born in Yorkshire, England, on October 17, 1961. He was awarded a First Class Honours degree in Applied Physics from Durham University, England in 1983. He then worked as a Systems Engineer at Marconi Radar Systems, where he became interested in optical fibre communication systems. In 1984 he was appointed as a University Lecturer at the University of Nottingham, England where he gained his Ph.D., "Transmission-line Modelling of Semiconductor Lasers," in 1988. In 1990 he moved to Australia to take up a position as a Senior Lecturer in the newly-formed Photonics Research Laboratory at the University of Melbourne, which is now part of the Australian Photonics Cooperative Research Centre. In January 1993 he was promoted to Associate Professor and Reader at the University of Melbourne.

Dr. Lowery has published more than 80 research papers in the fields of photonics and numerical modelling, and has one patent on the design of mode-locked lasers. His research interests include photonic CAD, mode-locked lasers, laser amplifiers, photonic switching, fibre video distribution, transmission-line modelling of electromagnetic fields, industrial ranging systems and semiconductor laser design. He is closely involved with the European Community's COST-240 project on Modelling and Measuring Advanced Photonic Telecommunications Components, and manages the projects '*Photonic CAD*' and '*Solitons and High-Speed Systems*' within the Australian Photonics Cooperative Research Centre. Dr. Lowery is a Chartered Engineer, a Member of the Institution of Electrical Engineers and a Member of the Institute of Electrical and Electronic Engineers.

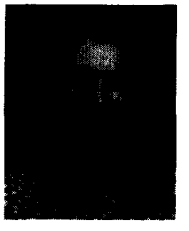

Dalma Novak (S'90–M'91) was born in Hungary on the 15th of April, 1967. In 1987 she graduated from the University of Queensland, Australia, receiving the degree of Bachelor of Engineering (Electrical) with First Class Honours. She received the Ph.D. degree from the same university in 1992. Her Ph.D. project investigated the dynamic behaviour of directly modulated semiconductor lasers. In January 1992 she was appointed as a lecturer in the Department of Electrical and Computer Engineering, University of Queensland. In September 1992 she joined the Photonics Research Laboratory (PRL) in the Department of Electrical and Electronic Engineering at the University of Melbourne as a lecturer. The PRL is a member of the Australian Photonics Cooperative Research Centre and she manages the Centre Project on Hybrid Optical/Microwave Communication Systems. Her research interests include high-speed semiconductor lasers, mode-locking, optical generation of microwave and millimetre-wave signals, optical fibre microcellular communication systems and low profile conformal antennas for integration with optical fibre feeds. Dr. Novak is a Member of the IEEE and is a Member of the IEEE Victorian Section Committee.